A COMBINED LIMIT CYCLE - ZERO MOMENT POINT BASED APPROACH FOR OMNI-DIRECTIONAL QUADRUPEDAL BOUNDING

ROMEO ORSOLINO*, MICHELE FOCCHI, DARWIN G. CALDWELL and
CLAUDIO SEMINI

Dept. of Advanced Robotics, Istituto Italiano di Tecnologia (IIT)
**E-mail: romeo.orsolino@iit.it*
https://www.iit.it/lines/dynamic-legged-systems-lab

In this paper we describe the steps that allowed us to realize real outdoor experiments of HyQ bounding at different speeds and performing omni-directional maneuvers. The strategy is composed of two parts: the first one is an offline optimization that finds a stable periodic limit cycle which represents the baseline bounding gait; the second part is a speed controller that adjusts online the main gait parameters based on the high-level speed commands coming from the external operator. In the tests HyQ reached a forward speed of $2.5m/s$, lateral speed of $1m/s$ and angular speed of $50deg/s$ in simulation and respectively $1m/s$, $0.5m/s$ and $30deg/s$ on the hardware experiments.

Keywords: bounding gait, quadruped legged locomotion, hydraulic robots, gait optimization, optimal control, direct methods

1. Introduction

Despite the extensive research on legged locomotion there exists still a relevant gap between the agility of quadrupedal animals and their robotic counterparts. From the hardware point of view this gap is due to the lack of resistant yet compliant limbs, high power/weight ratio actuators and precise sensors. From the software point of view, instead, one of the main shortcomings lies in the lack of a universal stability criterion that allows to plan joint trajectories and feed-forward torques in a computationally efficient manner and for arbitrary movements.

Related work: many implementations in the last decades have already shown legged robots with impressive dynamic capabilities in performing hops, jumps and dynamic gaits starting from Raibert's hoppers and quadrupeds.[1] Advanced studies on omni-directional bounding gait have been carried out on the Scout II[2,3] robot and, in simulation, on KOLT[4] and HyQ.[5] Recent improvements in the bounding gait have been obtained on the MIT cheetah which has achieved impressive results managing to online replan and jump obstacles while bounding and to gallop even in the presence of relevant changes in the terrain height.[6] Optimization based approaches to achieve agile motions such as bounding have also been shown on StarlETH.[7] An analysis on the benefits of an active spine for turning maneuvers while bounding has been carried out on the Bobcat-robot.[8]

The contribution of this paper lies in the combination of a Zero Moment Point (ZMP) based strategy for enhancing the lateral stability of a quadruped robot during the front/hind stance phases with the periodic limit cycle approach used to discover a stable bounding gait. This allows us to show real outdoor experiments of HyQ, IIT's 80 kg hydraulic torque-controlled quadruped robot[9] (Fig. 1), performing omni-directional bounding. A minor contribution is also a module for the online replanning of the feet trajectories given the trunk's state which we call *linear kinematic adjustment.*

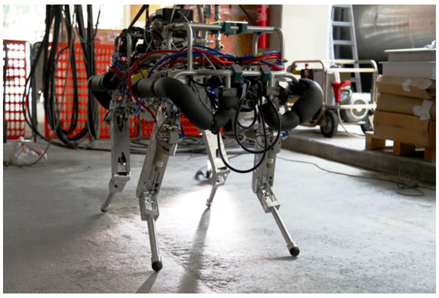

Fig. 1. HyQ, the hydraulic quadruped robot of IIT.

This document is organized in the following way: we illustrate in Section 2 a lower dimensional planar model of the robot used to achieve a stable periodic bounding gait. Section 3 describes the design of the linear speed and turning controllers. In Section 4 we present the results of the simulations and hardware experiments carried out on HyQ. In Section 5 it follows the final discussion where we also draft future development directions.

2. Baseline optimization

We employ the simplified planar dynamic model portrayed in Fig. 2(a). The state of the robot's center of mass (CoM), where we consider the lumped mass m of the robot to be placed, is defined by its planar coordinates ${}_{w}\mathbf{x}_{com} = [x, z, \theta]^T$. The base position is instead denoted by ${}_{w}\mathbf{x}_{b}$. The forces $\mathbf{F}_f = [F_{fx}, F_{fz}]^T$ and $\mathbf{F}_h = [F_{hx}, F_{hz}]^T$ represent the desired ground reaction forces (GRFs) of front and hind legs, respectively. Their lever arm with respect to the CoM of the trunk is denoted by $\mathbf{l}_f = [l_{fx}, l_{fz}]^T$ and

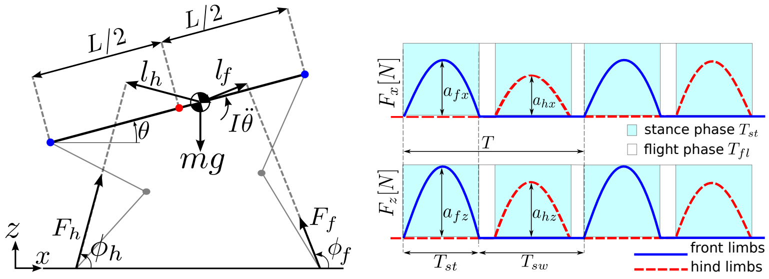

(a) (b)

Fig. 2. (a) Low dimensional dynamic model of HyQ in the sagittal plane; (b) impulse-shaped feed-forward forces at the feet.

$\mathbf{l}_h = [l_{hx}, l_{hz}]^T$. The resulting equations of motion are:

$$\begin{cases} m\ddot{x} = F_{fx} + F_{hx} \\ m\ddot{z} = -mg + F_{fz} + F_{hz} \\ I\ddot{\theta} = \mathbf{l}_f \times \mathbf{F}_f + \mathbf{l}_h \times \mathbf{F}_h = F_{fx}l_{fz} + F_{fz}l_{fx} + F_{hx}l_{hz} + F_{hz}l_{hx} \end{cases} \tag{1}$$

where I is the lumped inertia of the whole robot. If we assume the quantities $\mathbf{l}_f$ and $\mathbf{l}_h$ to have constant values $\mathbf{l}_f$, $\mathbf{l}_h$ then the equations 1 are therefore linear in the contact forces $\mathbf{F}_f$ and $\mathbf{F}_h$. We enforce the impulsive nature of these contact forces during the bounding gait by imposing, through a time-variant function $\mathbf{g}(t)$, $\mathbf{F}_f$ and $\mathbf{F}_h$ to take on an impulse-like shape defined by 4^{th} order Bézier curves as in Fig. 2(b). These curves fit well with the experimental data of the GRFs created by humanoids[10] and quadrupeds. The integral of the overall feed-forward forces over the stance time T_{st} are the impulses $\mathbf{J}_f$ and $\mathbf{J}_h$.

$$\mathbf{J}_f = \int_0^{T_{st}} \mathbf{F}_f(t)dt = \int_0^{T_{st}} \mathbf{g}(t)\mathbf{a}_f dt \quad \mathbf{J}_h = \int_0^{T_{st}} \mathbf{F}_h(t)dt = \int_0^{T_{st}} \mathbf{g}(t)\mathbf{a}_h dt \tag{2}$$

The impulses $\mathbf{J}_f = [J_{fx}, J_{fz}]^T$ and $\mathbf{J}_h = [J_{hx}, J_{hz}]^T$ for a fixed T_{st} depend only on the amplitude of the force profiles $\mathbf{a}_f = [a_{fx}, a_{fz}]^T$ and $\mathbf{a}_h = [a_{hx}, a_{hz}]^T$ (see Fig. 2(b)). The determination of the value of these constant amplitudes is the goal of subsection 2.1.

2.1. *Discovery of the periodic limit cycles*

We intend to solve a boundary value problem (BVP) where the optimization variables are $\mathbf{a}_f$ and $\mathbf{a}_h$ besides the initial pitch θ_0 and pitch rate $\dot{\theta}_0$. Moreover, we enforce periodicity by imposing the final and initial states $\mathbf{s}_T$ and $\mathbf{s}_0$ to be equal: $\mathbf{s}_0 = \mathbf{s}_T$. The state $\mathbf{s}$ is the concatenation of ${}_w\mathbf{x}_{com}$ and ${}_w\dot{\mathbf{x}}_{com}$: $\mathbf{s} = [{}_w\mathbf{x}_{com}^T, {}_w\dot{\mathbf{x}}_{com}^T]^T = [x, z, \theta, \dot{x}, \dot{z}, \dot{\theta}]^T$. Given the desired height at the apex of the flight phase z_{apex}, we can compute the expected swing time $T_{sw} = 2\sqrt{\frac{2z_{apex}}{g}}$ and the other dependent parameters of the gait such as the cycle time $T = T_{sw} + T_{st}$, the flight time $T_{fl} = \frac{T-2T_{st}}{2}$ and the duty factor $D = T_{st}/T$.

In the direct multiple-shooting approach[11] the goal is to discretize the states from $t = 0$ to $t = T$ into N sub-intervals $t = k/N$ with $k = 0, 1, 2, \ldots N$. $\mathbf{u}$ is nothing but the set of the amplitudes $\mathbf{a}_f$, $\mathbf{a}_h$ which remains constant throughout the cycle period $\mathbf{u} = [\mathbf{a}_f^T, \mathbf{a}_h^T]^T = [a_{fx}, a_{fz}, a_{hx}, a_{hz}]^T$. The state $\mathbf{s}$ is instead a $[6 \times N]$-dimensional vector $\hat{\mathbf{s}} = [\mathbf{s}_0 \ldots \mathbf{s}_k \ldots \mathbf{s}_N]$. The dynamic equations in 1 can then be expressed as $\mathbf{s}_{k+1} = \mathbf{f}(\mathbf{s}_k, \mathbf{u}_k)$. In our analysis we use $N = 400$ samples on a cycle time of $T = 0.4s$ for an integration step of $dt = 0.001s$.

The goal is to minimize the cost function $L(\theta_0, \dot{\theta}_0, \mathbf{u})$ over each gait cycle:

$$\mathbf{y}^* = \min_{\theta_0, \dot{\theta}_0, \mathbf{u}} L(\theta_0, \dot{\theta}_0, \mathbf{u}) = \min_{\theta_0, \dot{\theta}_0, \mathbf{u}} \sum_{k=1}^{N} (\theta_k^2 + \dot{\theta}_k^2 + \mathbf{u}_k^T \mathbf{u}_k) \tag{3}$$

s.t.:

(a) continuity: $\mathbf{s}_{k+1} = \mathbf{f}(\mathbf{s}_k, \mathbf{u}_k)$
(b) periodicity: $\mathbf{s}_0 = \mathbf{s}_T$
(c) Bézier force profile: $\mathbf{F}_k = \mathbf{g}_k \mathbf{u}_k$
(d) saturation: $u_{min} \leq \mathbf{u}_k \leq u_{max}$

The term $\mathbf{u}$ in the quadratic cost function $L(\theta_0, \dot{\theta}_0, \mathbf{u})$ is employed in order to limit the amplitude of the impulses and, as a consequence, the torque required to the actuators. The reason for adding θ_0 and $\dot{\theta}_0$ to the cost function stems from the need of respecting the friction cone constraint: even if a relevant trunk oscillation is a characterizing feature of the bounding gait we still want to avoid extreme motions of the pitch that may require too large horizontal forces to keep the bounding in place.

The constraint (c) is nonlinear because it describes the impulse-shaped profile of the feed-forward forces. The optimal control problem was therefore solved with the nonlinear solver IPOPT using the CasADi interface.[12]

We found a set of solutions $\mathbf{y}^*$ corresponding to different values of the input parameter T_{st} in the range between $50ms$ and $300ms$ and analyzed the stability of these different periodic limit cycles obtained (see Fig. 3 (a)). This analysis shows that all the eigenvalues λ_i of the discrete linearized Poincaré map have a magnitude larger than 1 ($\lambda_i > 1$) meaning that the found periodic limit cycles are open-loop unstable for all the analyzed duty factors D. The optimized impulses are then used as feed-forward torques at joint level where it is possible to show that the necessary stabilization can be performed by exploiting the active impedance in joint space. We do not report the details here for the sake of brevity.

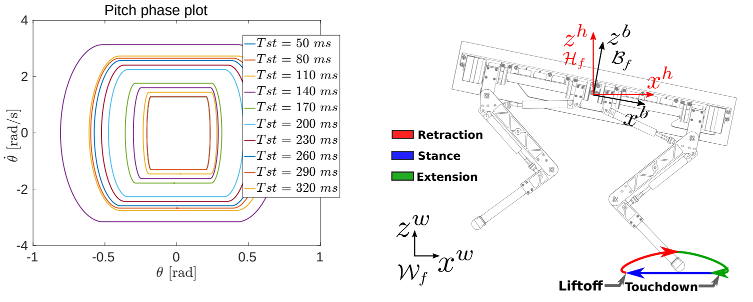

(a) (b)

Fig. 3. (a) Periodic limit cycles for different values of T_{st}; (b) feet trajectory generation.

3. Speed and turning control

The obtained desired foot, CoM and base trajectories $({}_w\mathbf{x}_f^d, {}_w\dot{\mathbf{x}}_f^d)$, $({}_w\mathbf{x}_{com}^d, {}_w\dot{\mathbf{x}}_{com}^d)$ and $({}_w\mathbf{x}_b^d, {}_w\dot{\mathbf{x}}_b^d)$ are computed in the *world frame* $\mathcal{W}_f$. They need to be mapped into the *base frame* $\mathcal{B}_f$ before they get fed into the inverse kinematics and finally become joint trajectories. We make use of an intermediate reference frame named *horizontal frame* $\mathcal{H}_f$ which shares the same origin and yaw angle with $\mathcal{B}_f$ but it is aligned with gravity $\mathbf{g}$. The mapping is therefore a cascade of a linear translation ${}_wt_b$ from $\mathcal{W}_f$ to $\mathcal{H}_f$, called *linear kinematic adjustment*, and a rotation ${}_bR_h$ from $\mathcal{H}_f$ to $\mathcal{B}_f$ called *angular kinematic adjustment* (first introduced in Barasuol *et al.*[13]). The peculiarity of this transformation lies in the use of the *actual state* of the robot rather than the desired state. In the case of the *linear kinematic adjustment* we will have:

$$\begin{cases} h\mathbf{x}_f^d = {}_w\mathbf{x}_f^d - {}_w\mathbf{x}_b \\ {}_h\dot{\mathbf{x}}_f^d = {}_w\dot{\mathbf{x}}_f^d - {}_w\dot{\mathbf{x}}_b \end{cases} \tag{4}$$

This allows to ensure e.g. the desired foot clearance even when the trunk is not in the expected configuration enhancing the tracking of the feet trajectories. Equation 4 requires the knowledge of the base position in $\mathcal{W}_f$. This is not easy to obtain, especially when slippage may occur or the flight phase may last slightly longer or shorter than expected. To mitigate the dependency on the state estimation we reset the world frame $\mathcal{W}_f$ to be coincident with $\mathcal{H}_f$ at the latest apex state (i.e. when ${}_h\dot{z}_b^h = 0$). In such way we neglect the accumulated errors of the past gait cycles (see Fig. 3(b)).

3.1. *Speed controller*

We implemented a speed controller that creates at each gait cycle an offset in the overall linear and angular momentum that propels the robot in the

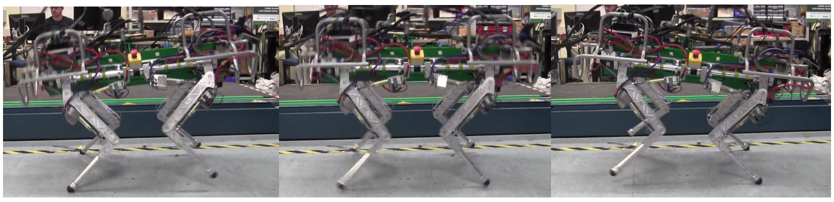

Fig. 4. HyQ bounding *in place* in IIT's lab. with a duty factor of $D = 0.45$

desired direction. The optimal values of $\mathbf{a}_i^*$ (where i is the leg index: $i = \{LF, RF, LH, RH\}$) are modified to $\mathbf{a}_i$ with the following strategy:

- angular speed control: $a_{iy} = a_{iy}^* + K_{d,\psi}(\dot{\psi}^d - \dot{\psi})/{}_h x_{f_i}$ where ${}_h x_{f_i}^d$ is the x coordinate of the i^{th} foot;
- forward and lateral speed control: $a_{ix,y} = a_{ix,y}^* + K_{d,\dot{\mathbf{x}}}({}_h\dot{\mathbf{x}}_b^d -_h \dot{\mathbf{x}}_b)$

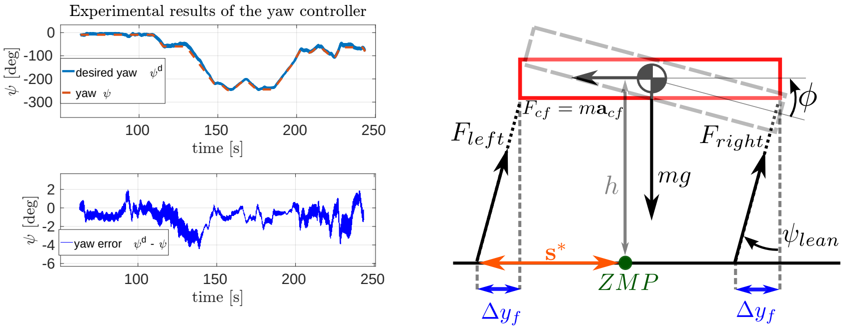

(a) (b)

Fig. 5. (a) Yaw controller performance from experimental data; (b) frontal section from the back of HyQ performing a turn to the right subject to centrifugal forces.

The higher the forward speed ${}_h\dot{x}_b \neq 0$ the more important it becomes to take the centrifugal acceleration a_{cf} into account (see Fig. 5(b)) $a_{cf} = \frac{{}_h\dot{x}_b{}^2}{r}$ where r is the instantaneous radius of curvature $r =_h \dot{x}_b/\dot{\psi}^d$. The quantity a_{cf} will cause a shift of the ZMP outwards with respect to the turn, thus reducing the lateral stability margin represented by the distance s between the ZMP and the foot along the support line of the double stance phase. This also results in unloading the internal leg during the turn. Our strategy consists in moving the feet laterally by an offset Δy_f to restore the desired lateral stability margin s^* and, as a consequence, to re-equilibrate the force distribution between the two stance legs. As a consequence of this offset $\Delta y_f = (a_{cf} h)/g$ the legs will take on a certain leaning angle:

$$\varphi_{lean} = atan(\frac{\Delta y_f}{h}) \qquad (5)$$

where h is the height of the CoM of the robot. The legs then align with the contact forces (whose lateral component compensates for a_{cf}) and no extra torque is applied on the Hip Abduction/Adduction joints (see Fig. 5(b)). Furthermore, it is favorable in terms of energy efficiency to roll the trunk by the same leaning angle[4] s. t. $\phi = \varphi_{lean}$. The legs, in this way, get aligned with the main axis of the frontal section of their manipulability ellipsoid.

4. Simulated and Experimental Results

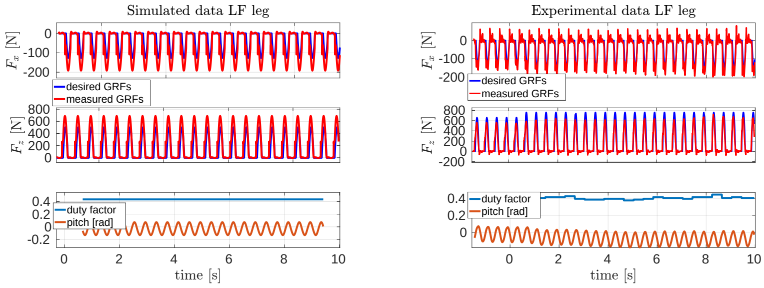

(a) Physics based simulation (b) Hardware experiments

Fig. 6. (a) simulated and (b) experimentally measured actual *vs.* desired GRFs in the two upper plots. Pitch and duty factor are instead shown in the lower plots.

Plots of the collected data both during simulated bounding and the hardware implementation are given in Fig. 6. The first two plots above show the frontal F_x and vertical F_z feed-forward forces and the corresponding ground reaction forces. The lower plot shows the pitch evolution and the measured duty factor. The use of the kinematic adjustment significantly mitigates the spike at touch down which is due to the non zero vertical velocity of the feet at the end of the legs extension phase. Thanks to the linear kinematic adjustment (Section 3) the effects on the feet of the trunk's dynamics are cancelled out and the vertical velocity of the feet is strongly reduced, resulting in a softer touch down.

The limit cycle periodicity of the pitch and the almost constant duty factor shown in the lower plot of Fig. 6 demonstrate that the system is successfully stabilized. In Fig. 4 you can see for three snapshots of HyQ bounding *in place* with a short flight phase in the middle frame.

4.1. *Yaw Controller*

Fig. 5(a) shows the performance of the yaw controller over a period of $180s$ during which the robot runs at constant speed of $1m/s$ and varies its angular velocity between $\pm 20deg/s$. In the lower plot it can be seen that the yaw error remains lower than 4 degrees throughout the time interval. Experimental results can be found in following link: https://youtu.be/005BMWixqsQ.

5. Conclusion and future works

We implemented a bounding gait of the HyQ quadruped robot which is able to reach a wide range of linear and angular speeds. In the future we intend to test the robustness of our approach with different ground stiffnesses and damping, with consistent changes in the terrains level and slopes.

References

1. M. H. Raibert, Trotting, pacing and bounding by a quadruped robot *Journal of Biomechanics* 1990.
2. S. Talebi, I. Poulakakis, E. Papadopoulos and M. Buehler, Quadruped Robot Running With a Bounding Gait *7th International Symposium on Experimental Robotics* 2000.
3. D. Papadopoulos and M. Buehler, Stable Running in a Quadruped Robot with Compliant Legs, in *IEEE International Conference on Robotics and Automation (ICRA)*, 2000.
4. L. R. Palmer and D. E. Orin, Intelligent control of high-speed turning in a quadruped *Journal of Intelligent and Robotic Systems: Theory and Applications* 2010.
5. X. Liu, C. Semini and I. Poulakakis, Active compliance hybrid zero dynamics control of bounding on HyQ *IEEE International Conference on Robotics and Biomimetics, ROBIO* 2015.
6. H.-W. Park and S. Kim, Quadrupedal galloping control for a wide range of speed via vertical impulse scaling *Bioinspiration & Biomimetics* 2015.
7. C. Gehring, S. Coros, M. Hutter, D. Bellicoso, H. Heijnen, R. Diethelm, M. Bloesch, P. Fankhauser, J. Hwangbo, M. Hoepflinger and R. Siegwart, Practice makes perfect: An optimization-based approach to controlling agile motions for a quadruped robot *IEEE Robotics & Automation Magazine* 2016.
8. M. Khoramshahi, A. Sprwitz, A. Tuleu, N. Ahmadabadi and A. Ijspeert, Benefits of an active spine supported bounding locomotion with a small compliant quadruped robot *IEEE Int. Conf. on Robotics and Automation (ICRA)* 2013.
9. C. Semini, N. G. Tsagarakis, E. Guglielmino, M. Focchi, F. Cannella and D. G. Caldwell, Design of HyQ - a hydraulically and electrically actuated quadruped robot *Proceedings of the Institution of Mechanical Engineers, Part I: Journal of Systems and Control Engineering* 2011.
10. J. Englsberger and C. Ott, Biologically Inspired Deadbeat control for running on 3D stepping stones *IEEE-RAS International Conference on Humanoid Robots (Humanoids)* 2015.
11. M. Diehl, H. G. Bock, H. Diedam and P.-B. Wieber, Fast Direct Multiple Shooting Algorithms for Optimal Robot Control *Fast Motions in Biomechanics and Robotics: Optimization and Feedback Control* 2006.
12. J. Andersson, J. Akersson and D. M., CasADi: A Symbolic Package for Automatic Differentiation and Optimal Control *Recent Advances in Algorithmic Differentiation* 2012.
13. V. Barasuol, J. Buchli, C. Semini, M. Frigerio, R. De Pieri and D. G. Caldwell, A reactive controller framework for quadrupedal locomotion on challenging terrain *International Conference on Robotics and Automation (ICRA)* 2013.